SIZE EFFECT IN ANCHORAGE BEHAVIOR

R. Eligehausen* and J. Ozbolt*

The results of the numerical analysis for pull-out tests on headed anchors with axisymmetric finite elements and nonlocal microplane model for concrete are presented. Based on the results of the numerical analysis and Bazant's size effect law a failure load formula is derived and compared with empirical failure load equations. Numerical results are in good agreement with experimental evidence and indicate a strong size effect which should be taken into account in current design practice.

INTRODUCTION

In engineering practice headed anchors are often used to transfer load into concrete structures. From experimental evidence it is clear that provided the steel strength of the stud is high enough, headed anchors fail by pulling a concrete cone. The failure is due to the failure of concrete in tension by forming a circumferential crack growing in so-called mixed mode (Eligehausen and Sawade (1)). As failure is due to concrete in tension, concrete tension properties as well as fracture energy have a dominant influence on the failure load, while concrete compression properties have a small influence on the failure load, but play an important role in the shape of the load-displacement curve (Ozbolt and Eligehausen (2)). Strong dependency between concrete fracture energy and failure load as well as experience from a number of pull-out tests indicates strong size effect. This means that the fracture is driven by the stored elastic energy that is released globally from the entire specimen at failure. This very important aspect of pull-out problem is still open. Due to this, the main objective of this study is to investigate the size effect in

* Universität Stuttgart, Institut für Werkstoffe im Bauwesen

pull-out problems using axisymmetric finite element analysis and nonlocal microplane model.

NUMERICAL ANALYSIS, FINITE ELEMENT DISCRETIZATION AND MATERIAL MODEL

In the numerical analysis four-nodes isoparametric finite elements with four integration points are used. The geometry of the specimen and typical finite element mesh is shown in Fig. 1. The size effect is analyzed using three geometrically similar specimens with the size increase by a factor of three. The geometry of the specimens is correlated with the embedment depth d. Three embedment depths are considered: d= 50, 150 and 450 mm. The distance between support and anchor is 3d, so that an unrestricted formation of the failure cone is possible. In all analyzed cases pulling out of the anchor is performed by prescribing displacements at the bottom of the head. Contact between anchor and concrete exists under the head of the stud only. To account for the restraining effect of the embedded anchor, the displacements of the concrete surface along the steel stud in the vicinity of the head are fixed in direction perpendicular to the load direction. Except supports, all other nodes at the concrete surface are supposed to be free.

The analysis is performed using nonlocal microplane model. Detailed description of the microplane model implemented into the finite element code is given by Bazant and Ozbolt (3). Material parameters are taken so that the resulting tension strength is approx. f_t= 3.0 MPa, fracture energy G_F= 0.1 N/mm and uniaxial compression strength approx. f_c = 40.0 MPa. Initial Young's modulus and Poisson's ratio are taken as E = 30000 MPa and ν = 0.20. Characteristic length in nonlocal analysis is taken as l = 12.0 mm.

RESULTS OF THE ANALYSIS

Load displacement curves for three different embedment depths are shown in Fig. 1. The displacement is monitored under the head. It can be seen that the displacement at failure load increasing with embedment depth. Assuming no size effect the failure loads should increase in proportion to d^2, that means by a factor of 9 when tripling the embedment depth. The results of the analysis show that the increase in failure load is much less (approximately by a factor of 5.7) which is a consequence of size effect.

Using Bazant's size effect law (Bazant (4)), the concrete cone failure load can be calculated by Eq. 1:

$$F_n = F_u B(1+d/d_0)^{-1/2} \qquad (1)$$

where F_n represents load at failure including size effect, F_u a failure load without size effect, d is embedment depth

while B and d_0 represent constants which are calculated from the linear regression analysis of the obtained failure loads. No size effect ultimate load F_u is calculated using a formula:

$$F_u = a \sqrt{f_c}\, d^2 \qquad (2)$$

where f_c represents concrete compression strength and a is a factor to calibrate calculated failure loads with the measured values and to assure the dimensional correctness of Eq. 2 . Eq. 2 is proposed by ACI 349, appendix B, (5) for the prediction of the concrete cone failure load.

In Fig. 2 the results of the analysis are plotted and compared with the size effect law (Eq. 1). The coefficient a in Eq. 2 is fixed such that the numerically obtained failure load for anchors with d= 50 mm is predicted correctly. From Fig. 2 is obvious that the results of the analysis agree rather well with the size effect law.

In Fig. 3 the results of the analysis are compared with different failure load equations. Plotted are the relative failure loads as a function of the embedment depth. The failure load for d= 150 mm is taken as reference value. The peak loads according to the size effect law (Eq. 1) and Eq. 2, which neglects the size effect, are shown. Furthermore, the failure loads according to the formula proposed by Eligehausen and Sawade (6), which is derived on the basis of linear fracture mechanics, and is of the form:

$$F_n = a_1 \sqrt{E G_F}\, d^{3/2} \qquad (3)$$

are also plotted. In Eq. 3 a_1 is a constant. The fracture loads predicted by Eq. 3 agree rather well with test results (6). From Fig. 3 it is clear that a formula that does not take into account the size effect (such as Eq. 2 proposed by ACI 349) underestimates the failure loads for small embedment depths and is unconversative for larger embedment depths. The agreement between the formula derived on the basis of size effect and the formula based on linear fracture mechanics is good in the entire embedment range.

The relative shape of the fracture cone for three different embedment depths is plotted in Fig. 4. The failure cone slopes after the peak load are estimated from the results at peak load, marked in the figure. The ratio diameter of the failure cone to embedment depth decreases with increasing anchorage depth. This agrees qualitatively with test results (1). Therefore the effective relative cone surface area decreases with increasing embedment depth, what is a consequence of the size effect.

The distribution of the tensile stresses perpendicular to the failure cone surface are shown in Fig. 5 as a function of the ratio l_h/l_{hmax} where l_h represents the distance from the anchor and l_{hmax} is the failure cone radius taken from Fig. 4. These distributions, which are estimated from the results of the numerical analysis, are more parabola like in the case of smaller embedments and more triangular like in the case of larger embedments. This is again a consequence of the size effect.

CONCLUSIONS

The results of the present numerical analysis indicates a significant size effect on the concrete cone failure load of headed anchors embedded in large concrete blocks. The failure loads increase approximately in proportion to $d^{3/2}$. This is in agreement with experimental evidence (1). Prediction formula which do not take into account the size effect, such as the formula proposed by ACI 349 (5), overestimate the failure load for large embedment depths. The size effect is due to the fact that the elastic energy at peak load is released from the entire structure and as a consequence the effective relative failure load surface as well as the area under the tensile stress distribution decrease with increasing embedment depth. The size effect on anchor failure loads should be taken into account in design practice.

REFERENCES

(1) Eligehausen, R. and Sawade, G., "Analysis of Anchoring Behaviour (Literature Review)", "Fracture Mechanics of Concrete Structures" - RILEM Report. Edited by L.Elfgren, Chapman and Hall, 1989.

(2) Ozbolt, J. and Eligehausen, R. , "Numerical Analysis of Headed Studs Embendded in Large Plain Concrete Blocks", Proceedings of the 2nd International Conference on "Computer Aided Analysis and Design of Concrete Structures". Edited by N.Bicanic and H.Mang, Pinerdige Press, UK, 1990.

(3) Bazant, Z.P. and Ozbolt, J., "Nonlocal Microplane Model for Fracture, Damage and Size Effect in Structures", Northwestern University, Center for Concrete and Geomaterials, Report No. 89-10/498n, 1989.

(4) Bazant, Z.P., Journal of Eng. Mech., ASCE, Vol. 110, No.4, 1984, pp. 518-535.

(5) ACI 349-76: Code Requirements for Nuclear Safty Related Concrete Structures. ACI Journal, Aug. 1978.

(6) Eligehausen, R. and Sawade, G., "A Fracture Mechanics Based Description of the Pull-out Behavior of Headed Studs Embedded in Concrete ", "Fracture Mechanics of Concrete Structures" - RILEM Report. Edited by L.Elfgren, Chapman and Hall, 1989.

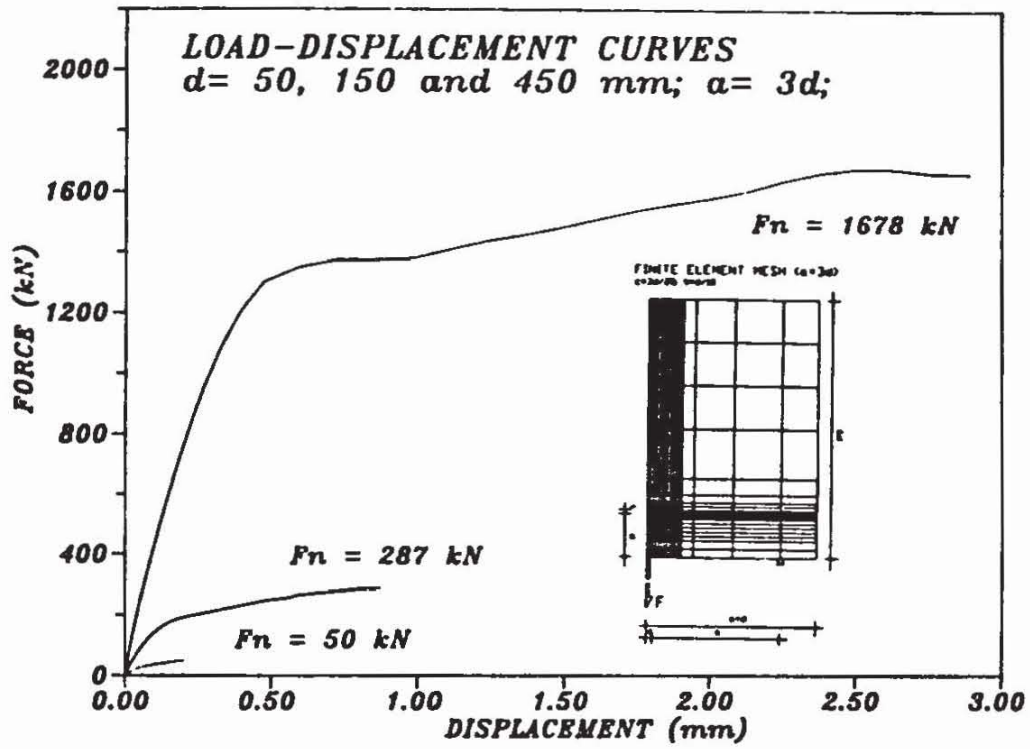

Figure 1 Load-displacement diagrams and FE mesh

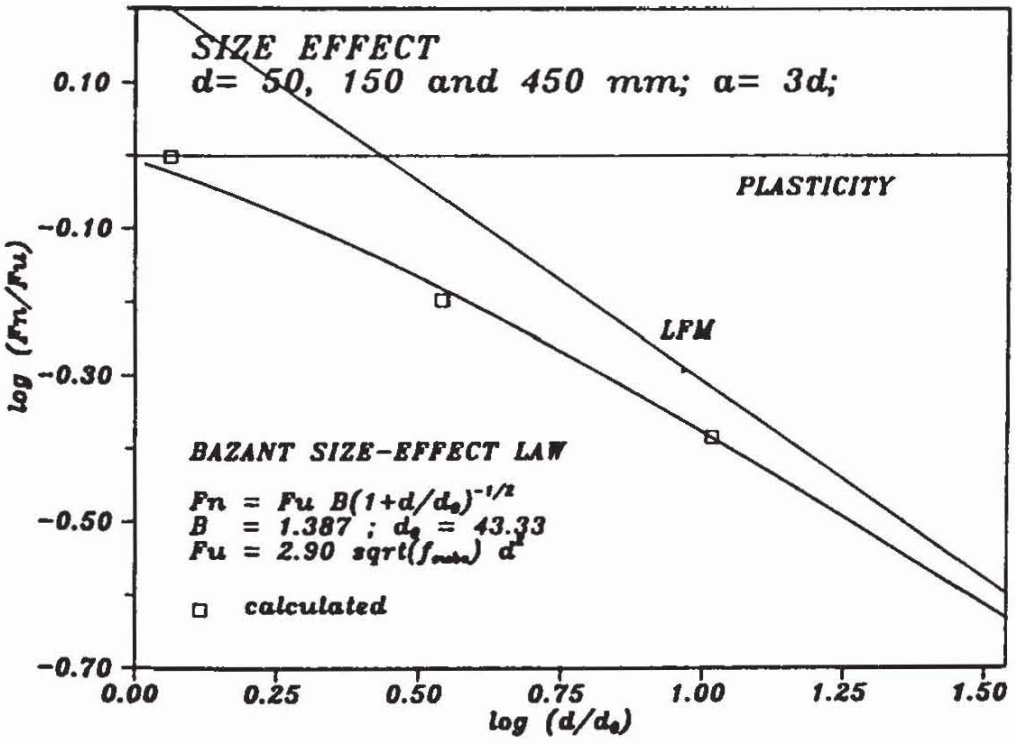

Figure 2 Comparision between size effect law and calculated results

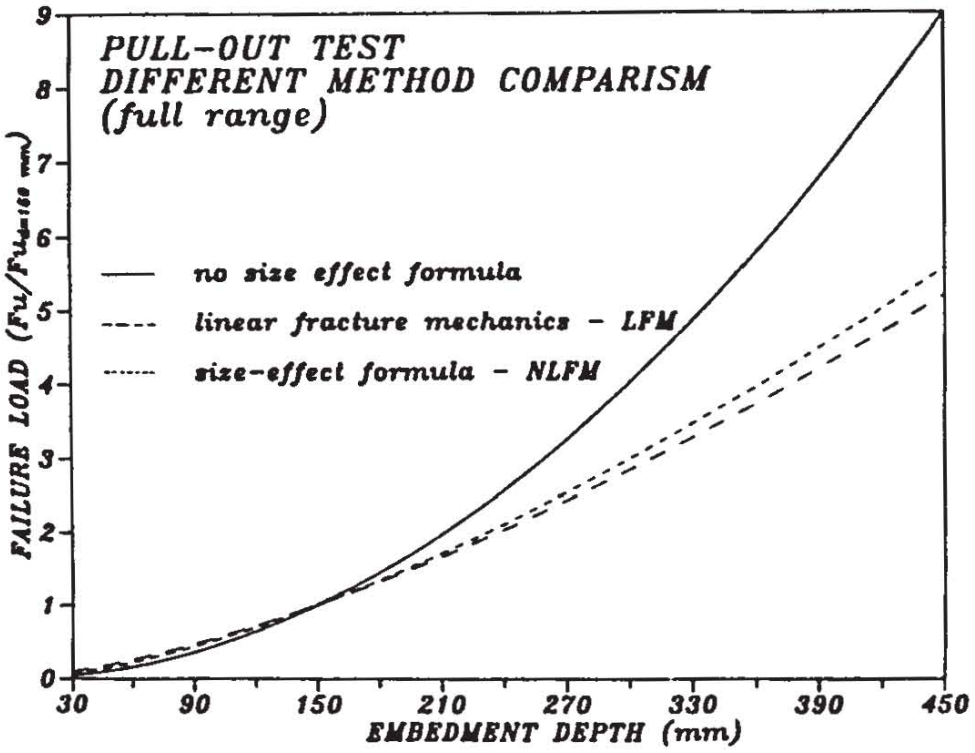

Figure 3 Prediction of the failure loads using different methods

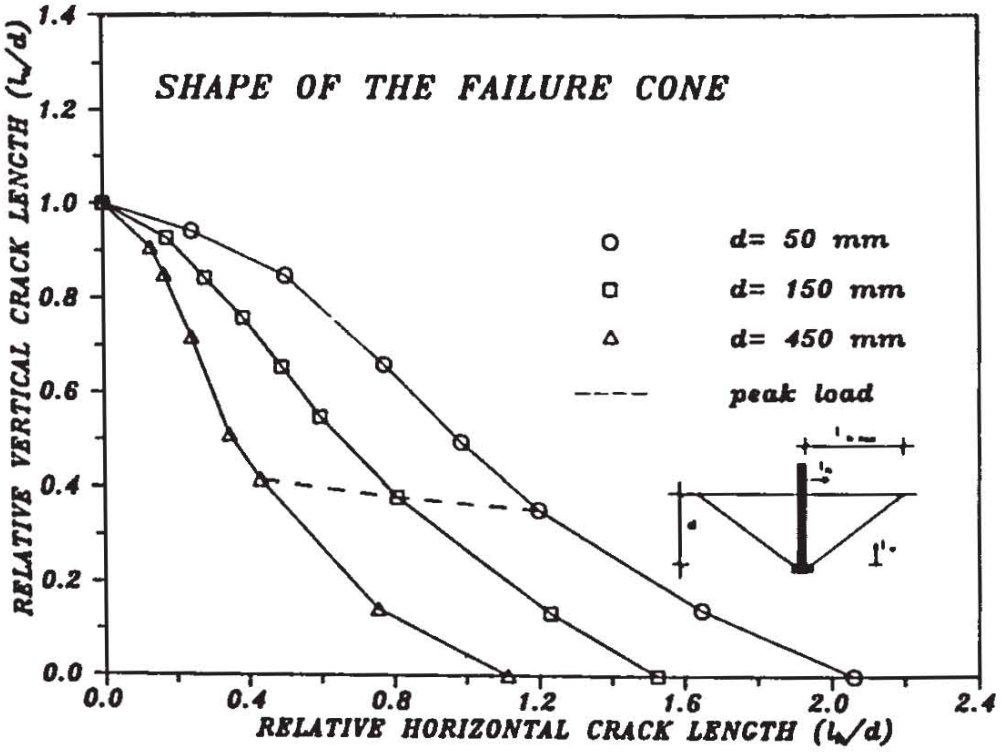

Figure 4 Shape of the failure cone surface area

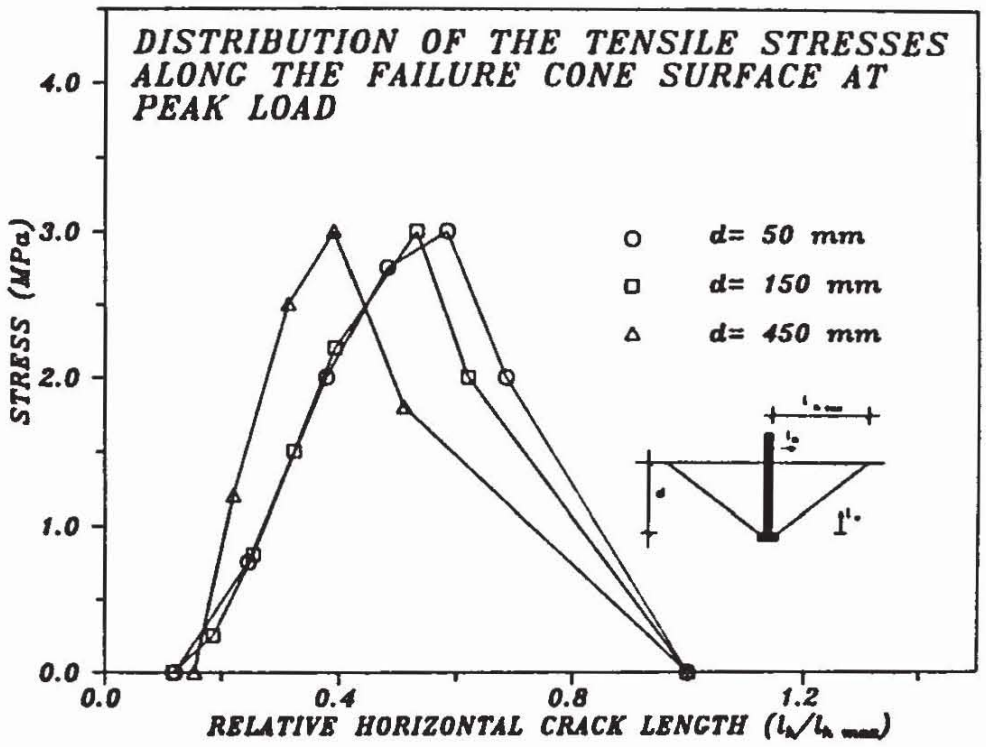

Figure 5 Tensile stress distribution along the cone surface